

# Simulated internal quantum deficiency of induced junction photodiodes

Trinh Tran<sup>1</sup> and Jarle Gran<sup>1</sup>

<sup>1</sup>Justervesenet, Kjeller, Norway,

Corresponding e-mail address: ttr@justervesenet.no

The paper presents a study of the internal quantum deficiency of the predictable quantum photodetector (PQED) using 3D device simulation. It is shown that surface recombination velocity and fixed oxide charge density are the key parameters that have to be optimised in an effort to develop improved PQED photodiodes.

## INTRODUCTION

The PQED is accepted as a new primary standard for radiant power measurement due to its low loss and predictable response [1]. This detector is constructed from two self-induced p-n junction photodiodes. The p-n junction is formed by the fixed charge between a dielectric surface layer and a silicon substrate. By optimising materials and fabrication processes to minimize surface recombination and to maximize fixed charge density, it is suggested that PQED photodiode with internal quantum deficiency (IQD) below ppm can be constructed [2]. Work is ongoing to develop improved induced junction photodiodes in the common European 18SIB10 *chipS*-CALe project [3], where expected response from simulations are an essential input to achieve the goal.

## RESULTS AND DISCUSSION

The photodiode response is studied by using 3D simulation model developed in Genius Device Simulator from Cogenda [4]. The simulation structure is shown in Fig. 1. In order to save time and memory, only 1/8 of the real device is simulated and the symmetry boundary conditions are applied to obtain the response to the whole photodiode structure. The simulation structure consists of a low doped p-type silicon substrate with an oxide passivation layer on the surface which induces a fixed surface charge density  $Q_f$  at the silicon-oxide interface. The silicon substrate thickness is 500  $\mu\text{m}$ . The electrodes are defined as  $p^+$  doping and  $n^+$  doping areas that have the width of 100  $\mu\text{m}$  and separation distance of 300  $\mu\text{m}$ . The rear side is also implemented with a  $p^+$  doping that has the same doping concentration as the

front side contact doping. The fixed simulation parameters used here are shown in the Table 1.

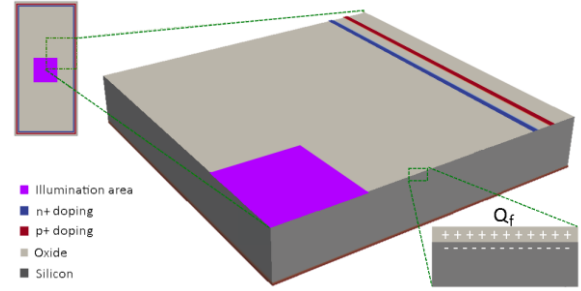


Figure 1. Simulation structure of a PQED photodiode.

Table 1. Simulation parameters.

Parameters	Value
Simulation structure	6mm×6 mm
Illumination area	1.5mm×1.5mm
Substrate doping concentration	$1.5 \times 10^{12} \text{cm}^{-3}$
Shockley-Read-Hall bulk lifetime	$2.9 \times 10^{-3} \text{s}$
Temperature	300K

IQD caused by charge carrier recombination is calculated by the following equation:

$$IQD = Rec/G_{opt} \quad (1)$$

where  $G_{opt}$  is the total rate of optically generation and  $Rec$  the total recombination rate of e-h pairs. Both  $G_{opt}$  and  $Rec$  can be extracted from simulation. We choose to decompose the total recombination in surface recombination and bulk recombination.

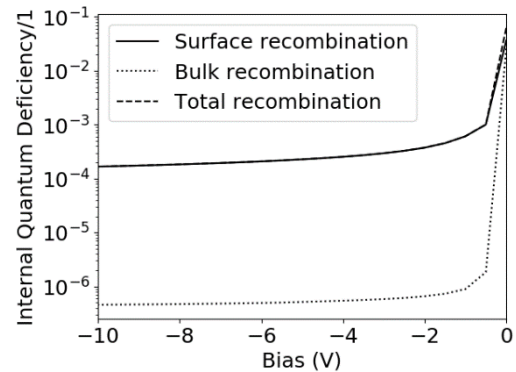
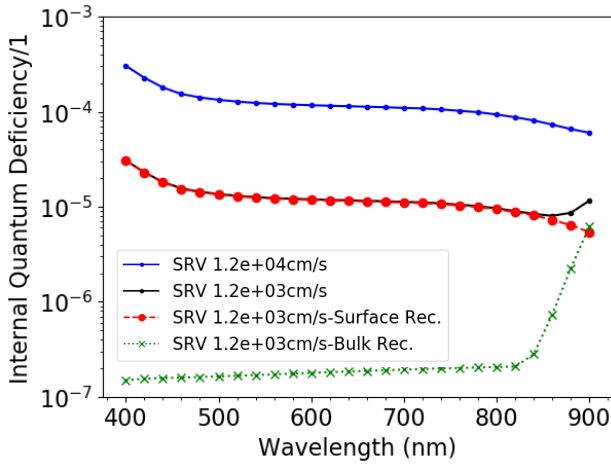


Figure 2. IQD response of photodiode with reversed bias.

A plot of typical IQD response of PQED photodiode with illumination at 450 nm with reversed bias is shown in Fig. 2. The simulation is done using  $Q_f$  of  $6 \times 10^{11} \text{ cm}^{-2}$ , surface recombination velocity (SRV) of  $1.2 \times 10^4 \text{ cm/s}$  and absorbed optical power of  $1 \times 10^{-4} \text{ W}$ . By applying reversed bias up to  $-10 \text{ V}$ , the total IQD is reduced from  $6.2 \times 10^{-2}$  to  $1.7 \times 10^{-4}$  with the largest reduction from 0 V to  $-0.5 \text{ V}$  bias.



**Figure 3.** IQD as a function of wavelength of photodiode at two values of SRV.

Fig. 3 shows the spectrally dependent IQD with two different values of SRV with  $-10 \text{ V}$  reversed bias at room temperature. The simulations are performed with  $Q_f$  equals  $6.5 \times 10^{11} \text{ cm}^{-2}$  and SRV is varied from  $1.2 \times 10^3 \text{ cm/s}$  to  $1.2 \times 10^4 \text{ cm/s}$ . It is seen that IQD changes one order of magnitude when the SRV is varied with one order of magnitude. Additionally, the decomposed IQD caused by SRV and bulk recombination at SRV  $1.2 \times 10^3 \text{ cm/s}$  are shown in the plot. With the parameter values of the SRV and bulk lifetime used here it is evident that the SRV limits the IQD over the whole visible spectral range.

The dependence of total IQD loss with 0 V reverse bias as a function of absorbed optical power with different  $Q_f$  is shown in Fig. 4. Fixed SRV value of  $1.2 \times 10^4 \text{ cm/s}$  and illumination wavelength of 450 nm are used as input parameters for the simulations. The same trend is observed on all curves. IQD does not change much at low power level. At higher absorbed optical power, IQD shows a sharp increase and becomes saturated. At low absorbed optical power, there is not much loss that comes from bulk recombination. As absorbed optical power increases, bulk recombination begins to contribute more to the total IQD until it reaches its saturated value at very high optical power.  $Q_f$  also has a field effect passivation influence of the surface, but this effect saturates with charge density  $2 \times 10^{12} \text{ cm}^{-2}$ .

Above this value we see little influence of increasing the fixed charge from a passivation point of view, but a slight increase in linearity is still observed (not shown).

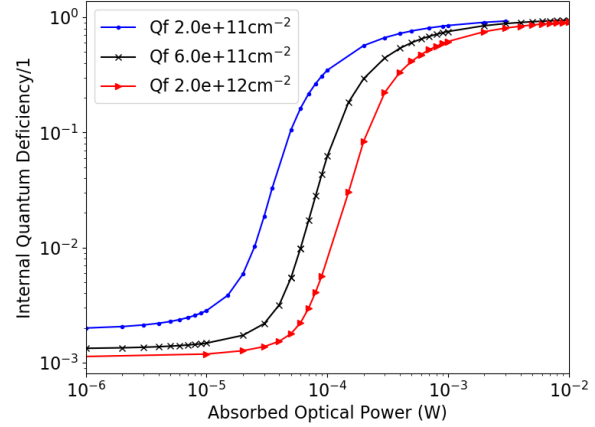


**Figure 4.** IQD as a function of absorbed optical power with different  $Q_f$ .

## CONCLUSIONS

The PQED spectrally dependent IQD is limited by the SRV whereas the fixed oxide charge  $Q_f$  limits the linearity of the photodiode. High  $Q_f$  improves the performance of the photodiodes with lower IQD and better linearity. The photodiodes should be operated with sufficient bias for low IQD. However, IQD below 0.1% losses can be achieved with unbiased diodes at low power levels.

## ACKNOWLEDGMENT

This work has received funding from the EMPIR programme co-financed by the Participating States and from the European Union's Horizon 2020 research and innovation programme.

## REFERENCES

1. I. Müller *et al.*, "Predictable quantum efficient detector: II. Characterization and confirmed responsivity," *Metrologia*, vol. 50, no. 4, pp. 395–401, Jul. 2013, doi: 10.1088/0026-1394/50/4/395.
2. T. S. Stokkan, H. Haug, C. K. Tang, E. S. Marstein, and J. Gran, "Enhanced surface passivation of predictable quantum efficient detectors by silicon nitride and silicon oxynitride/silicon nitride stack," *J. Appl. Phys.*, vol. 124, no. 21, p. 214502, Dec. 2018, doi: 10.1063/1.5054696.
3. J. Gran, Publishable Summary for 18SIB10 chipS.CALe. Zenodo, Jun. 2019. <http://doi.org/10.5281/zenodo.354567>.
4. <https://www.cogenda.com/>.